CHIN. PHYS. LETT. Vol. 35, No. 12 (2018) 123701

Sub-Doppler Laser Cooling of ^{23}Na in Gray Molasses on the D_2 Line *

Zhenlian Shi(师振莲)[1,2], Ziliang Li(李子亮)[1,2], Pengjun Wang(王鹏军)[1,2**], Zengming Meng(孟增明)[1,2], Lianghui Huang(黄良辉)[1,2], Jing Zhang(张靖)[1,2**]

[1]*State Key Laboratory of Quantum Optics and Quantum Optics Devices, Institute of Opto-electronics, Shanxi University, Taiyuan 030006*

[2]*Collaborative Innovation Center of Extreme Optics, Shanxi University, Taiyuan 030006*

(Received 14 September 2018)

We report on the efficient gray molasses cooling of sodium atoms using the D_2 optical transition at 589.1 nm. Thanks to the hyperfine split about 6Γ between $|F' = 2\rangle$ and $|F' = 3\rangle$ in the excited state $3^2P_{3/2}$, this atomic transition is effective for the gray molasses cooling mechanism. Using this cooling technique, the atomic sample in $F = 2$ ground manifold is cooled from 700 μK to 56 μK in 3.5 ms. We observe that the loading efficiency into magnetic trap is increased due to the lower temperature and high phase space density of atomic cloud after gray molasses. This technique offers a promising route for the fast cooling of the sodium atoms in the $F = 2$ state.

PACS: 37.10.De, 37.10.Gh, 67.85.−d DOI: 10.1088/0256-307X/35/12/123701

Ultracold atomic gases offer a remarkably rich platform[1] to enhance our understanding of numerous interesting phenomenon, such as coherent manipulation of many body states and their dynamics using quantum gases in optical lattices,[2−5] spin orbit coupling to topological matter,[6−11] and ultracold association molecules to study the long range dipole-dipole interaction and ultracold chemistry.[12−14] New cooling techniques are developed continuously to produce an atomic sample with a large atom number and lower temperature, such as 3D Raman sideband cooling[15−17] and electromagnetically induced transparency (EIT) cooling[18,19] in site-resolved imaging for Fermi atoms in optical lattice, and direct laser cooling of rubidium to quantum degeneracy in two-dimensional optical lattice.[20]

Cooling neutral atoms to ultracold temperatures usually starts with a magnetic-optical trap (MOT), and then transfers to optical trap or magnetic trap for efficient evaporative cooling. Sub-Doppler laser cooling is a powerful tool to decrease the temperature of a three-level atomic system below the Doppler temperature $\hbar\Gamma/2k_{\rm B}$, where $\hbar$ and $k_{\rm B}$ are the reduced Plank constant and the Boltzmann constant, and Γ is the natural line width of atomic transition.[21−23] This technique greatly increases the phase space density of the atomic cloud, resulting in the higher transfer efficiency to the trap and clearly leading to a gain in the final atom number after evaporative cooling. Gray molasses (GM) cooling is a special method for sub-Doppler laser cooling, which takes advantage of polarization gradient cooling and velocity selective coherent population trapping.[24]

In the 1990s, GM cooling was proposed in Ref. [25], in which the fluorescence rate of the trapped atoms is strongly reduced, and was then demonstrated experimentally on cesium[26−28] and rubidium[29] within the D_2 transition. More recently, GM cooling was realized on many atomic species, including alkali atoms ^{40}K,[30,31] ^{7}Li,[32] ^{39}K,[33,34] ^{6}Li,[31,35] ^{23}Na,[36] ^{41}K,[37] and metastable atom ^{4}He,[38] which was operating on the blue detuning of the D_1 transition with more resolved energy spectrum. The cooling technique was also implemented on the D_2 transition to cool ^{40}K to 50 μK with red-detuned laser,[39] and cool ^{87}Rb to 4 μK with blue-detuned laser.[40] It has been proven experimentally that the GM cooling leads to substantial advantages in terms of lower temperature and higher phase-space density. In the GM cooling mechanism, dark and bright states are the coherent superposition of Zeeman sublevels in the ground hyperfine manifold.[31] The bright state energy is spatially modulated, giving a polarization gradient cooling like a standard red detuned molasses. Atoms with higher energy in dark states could be coupled to the bright states by motion induced coupling and then could be cooled down in the polarization gradient cooling. Meanwhile, atoms with lower energy are trapped in dark space, which prevents heating induced by light-assisted collisions.

In this Letter, we report on an experimental study of sodium atoms cooled in six beams GM on the blue side of the D_2 transition $|F_{\rm g} = 2\rangle \rightarrow |F_{\rm e} = 2\rangle$, as shown in Fig. 1(a). Thanks to the much reduced fluo-

*Supported by the National Key Research and Development Program of China under Grant No 2016YFA0301602, the National Natural Science Foundation of China under Grant Nos 11474188 and 11704234, the National Key Research and Development Program of China under Grant No 2018YFA0307601, the Fund for Shanxi '1331 Project' Key Subjects Construction, and the Program of Youth Sanjin Scholar.

**Corresponding author. Email: jzhang74@sxu.edu.cn; pengjun_wang@sxu.edu.cn

© 2018 Chinese Physical Society and IOP Publishing Ltd

rescence rate in GM compared to the bright molasses cooling, we are able to capture cold and dense atomic cloud of 3×10^8 atoms at temperature of 56 μK. After the GM phase, atoms in $|F = 2, m_F = 2\rangle$ are transferred to an optically plugged quadrupole trap, where F is the total angular momentum and m_F is its projection. We observe that the loading efficiency is increased to 70% due to the lower temperature and high phase space density of atomic cloud using the GM technique. We also show significant evidence of the atom's temperature and number after a short RF-induced evaporative cooling as a function of the two-photon Raman detuning in GM phase.

In the experiment, the laser light (at 589 nm) is produced by frequency doubling a master oscillator power amplifier (MOPA) system. First, the laser beam (at 1178 nm) of 23 mW from external cavity diode laser (ECDL) is seeded to a Raman fiber amplifier (RFA), to be amplified to 7 W and transferred to the SHG unit for second harmonic generation (SHG) modules. We obtain 3.3 W of output power at 589 nm, which is sufficient for cooling and trapping of ^{23}Na in experiment. This single laser source supplies the coherence between the two frequencies to generate the long-lived dressed dark states in GM cooling. The frequency of output beam is stabilized at $|F_g = 2\rangle \rightarrow |F_e = 3\rangle$ by the saturated absorption spectroscopy. The cooling and repumping laser beams are obtained using acousto-optic modulators (AOMs) in double pass configuration.[41] Here, the AOMs are acting as fast switches, and frequency and intensity tuners. The laser beams of the cooling and repumping laser are then combined by a polarization beam splitter (PBS) and delivered to the science cell by polarization maintaining optical fibers; as shown in Fig. 1(b). They are then expanded to 25 mm for MOT beams and distributed to the three pairs of σ^+-σ^- counter-propagating configuration.

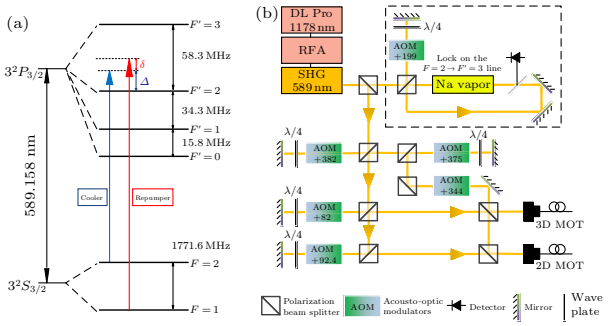

Fig. 1. (a) Sodium cooling scheme on the D_2 line. The cooling beam (blue) is blue detuned by Δ from the $|F_g = 2\rangle \rightarrow |F_e = 2\rangle$ transition, and the repumping beam (red) is blue detuned by $\Delta + \delta$ from the $|F_g = 1\rangle \rightarrow |F_e = 2\rangle$ transition, where $F_g(F_e)$ is the ground-excite state level. Here, δ denotes the two-photon Raman detuning. (b) Sketch of the optical setup for cooling sodium, and the dashed box represents the setup for saturated absorption spectroscopy.

Sodium atoms are loaded from a two-dimensional magnetic-optical trap and trapped by a dual-operation three-dimensional magnetic-optical trap (3DMOT) operating on the D_2 transition introduced in Refs. [42,43], in which two laser frequencies are used, one is tuned to the $|F_g = 2\rangle \rightarrow |F_e = 3\rangle$ transition with a red detuning 34 MHz for cooling and the other one is tuned to the $|F_g = 1\rangle \rightarrow |F_e = 2\rangle$ transition with a red detuning 57 MHz for repumping. In the 3DMOT, almost the same number of atoms are in the $F = 1$ and $F = 2$ states, and the total number is about 7.3×10^9. The temperature is about 700 μK. At the end of 3DMOT loading, the compressed magnetic optical trap (CMOT) is used to increase the density, in which the magnetic field gradient is ramped from 4 G/cm to 10 G/cm in 50 ms.

To decrease the temperature, the GM phase is applied for a duration time 3.5 ms after the magnetic field is switched off in $\simeq$ 100 μs. Here, we define the detuning of the cooling frequency from the $|F_g = 2\rangle \rightarrow |F_e = 2\rangle$ transition as the principal (one-photon) laser detuning Δ in the range of 1Γ–5Γ ($\Gamma = 2\pi \times 9.79$ MHz is the natural linewidth of the D_2 line), and the frequency difference between the cooler f_C and the repumper f_R as the two-photon Raman detuning $\delta = f_R - f_C - 1771.6$ MHz. During the molasses time t, the cooling and repumping beams are detuned to desired values and the intensity of two laser beams is reduced. At the end of the GM phase, an absorption image is applied to measure the temperature and number of the atomic cloud after a few ms of time of flight (TOF).

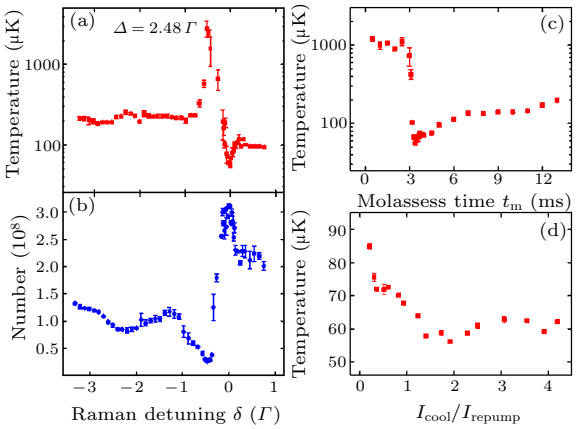

Fig. 2. (a) The temperature (red squares) and (b) number (blue circles) of atomic sample after GM with time $t = 3.5$ ms as a function of two-photon Raman detuning in the case of $\Delta = 2.48\Gamma$. The temperature after GM at the fix principal detuning $\Delta = 2.48\Gamma$ and Raman detuning $\delta = 0$, as functions of (c) the pulse duration time t and (d) the intensity ratio I_{cool}/I_{repump} of the Raman cooling pulse at a constant intensity $I_{repump} = 5I_{sat}$, where $I_{sat} = 6.26\,\text{mW/cm}^2$. The data points show the average of three experimental measurements, with error bars corresponding to the standard deviation of the mean.

We first study the effect of GM cooling for different experimental parameters with the fixed principal

detuning $\Delta = 2.48\Gamma$ (red detuned 34 MHz on the transition of $|F_g = 2\rangle \rightarrow |F_e = 3\rangle$, which means that it is the blue detuning 24.3 MHz for $|F_g = 2\rangle \rightarrow |F_e = 2\rangle$), such as two-photon Raman detuning, duration time of GM and the intensity ratio, as shown in Fig. 2.

The atomic sample temperature and number after the GM are observed as a function of two-photon detuning δ and a Fano-like profile at the atom temperature due to the interference of different excitation processes, accompanied by a sharp change in the number of cooled atoms; as shown in Figs. 2(a) and 2(b). Firstly, we focus on the case of the zero Raman detuning $\delta = 0$, where we find that the temperature minimum of $T = 56\,\mu$K is reached. The maximum number about 3.1×10^8 of the atomic cloud is obtained by the GM with a phase space density (PSD) of 1.3×10^{-6}, which means that in the case the atoms in dark spaces are maximally coupled to bright states at the bottom of energy hills and this induces a peak in the atom number in Fig. 2(b). The motion coupling between dark states and bright states is velocity selective, thus the atoms with higher velocity could be coupled to bright states and re-cooled by the Sisyphus cooling, and the coldest atoms will accumulate in the dark spaces with less interaction with the light field. The GM cooling mechanism is working in this case and could cool the atoms to lower temperature than the bright molasses on the D_2 line. For slightly red detuned at $\delta = -0.5\Gamma$, a heating peak is observed, which means that in the case the atoms in dark states have more energy than those in bright states and will gain kinetic energy when they couple to bright states at the top of energy hills. This mechanism leads a strong heating, and the temperature increases from 700 μK (the MOT temperature) to about 2 mK, accompanied by a significant loss of atom number during the molasses phase, which is the inverse of the Sisyphus cooling. In addition to the sharp dip and peak in atom temperature and number close the resonance $\delta = 0$, we notice that more atoms with lower temperature are captured in the case of $\delta > 0$ compared with that at the red detuning $\delta < 0$. This phenomenon is corrected and the main component of the dark state is lower than that of the bright state in the detuning $\delta > 0$, and more atoms could be trapped in dark states with lower temperature.

The temperature after the GM is plotted as a function of the duration time t_m in Fig. 2(c). The temperature decreases immediately at about 3 ms and reaches the minimum value at about 3.5 ms where a steady state is built, and then increases slowly with a longer duration. The observation of no noticeable cooling effect at first 3 ms is attributed to the small misplacement between the center of magnetic trap and the position of the atom cloud, which is designed for better loading in the MOT phase to avoid atoms loss. Figure 2(d) shows the temperature as a function of the ratio between cooler and repumper intensities $I_{\rm cool}/I_{\rm repump}$. We find a nearly linearly decrease at the initial regimes and a minimal temperature of $\sim 56\,\mu$K reached at the ratio of 2, and a slightly increase with more cooling power. This may be understood from the induced light shift in the dressed state picture.[32] In the case of fixed frequency, the atoms remained in dark states distribute the spatial variation of the standing wave and loss how much energy depending on the difference of light shift between the entry and departure points, as in the behavior of bright molasses.

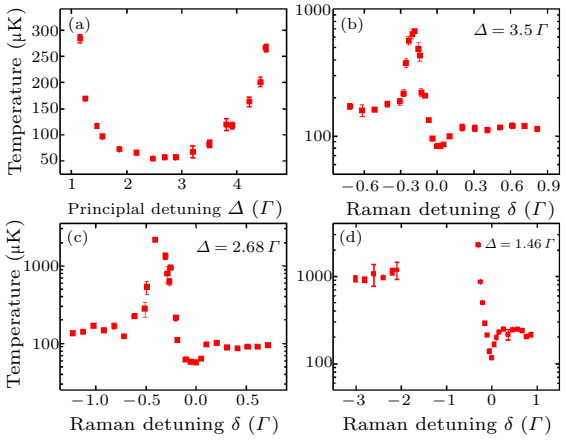

Fig. 3. (a) The minimum temperature obtained after GM as a function of the principal detuning Δ. The atom temperature of ^{23}Na after $t = 3.5$ ms of GM cooling as a function of two-photon Raman detuning in the case of (b) $\Delta = 3.5\Gamma$, (c) $\Delta = 2.68\Gamma$ and (d) $\Delta = 1.46\Gamma$.

We also measure the atom temperature after the GM with different one-photon detunings for $1\Gamma < \Delta < 5\Gamma$ on the blue side of the transition of $|F_g = 2\rangle \rightarrow |F_e = 2\rangle$, as shown in Fig. 3. This shows that the minimal temperature could reach $\sim 55\,\mu$K for $\Delta = 2.48\Gamma$, and increases on both sides. This behavior can be attributed to the chosen structure in GM: the energy separation between $|F_e = 2\rangle$ and $|F_e = 3\rangle$ in excite states is about 5.9Γ, thus for higher Δ, the upper state may start to play a role. As mentioned in Ref. [40], the closed transition of $|F_g = 2\rangle \rightarrow |F_e = 3\rangle$ contributes to the inefficiency of the GM cooling. This phenomenon is different from that of GM on the D_1 optical transition, in which the reached temperature is weakly dependent on the one-photon laser detuning.

The measured temperatures after GM with different one-photon detunings as a function of the two-photon Raman detuning δ are shown in Figs. 3(b)–3(d). For each value of Δ, the minimum temperature is obtained on $\delta \approx 0$, similar to the report in earlier experiments. In the case of $\Delta = 1.46\Gamma$, there is a very wide heating window and the temperature is very higher at the red detuning, where the repumper is in close resonance with the atomic transition of $|F_g = 1\rangle \rightarrow |F_e = 2\rangle$; as shown in Fig. 3(d). During

optimizing of the GM, we find that the stray magnetic field and misalignment of the laser beams affects the attained minimal temperature of the GM phase. Here, the three pairs of coils are used to produce XYZ bias fields to compensate for the stray field.

The most evident advantage of the GM is to obtain a large number of atoms with lower temperature for loading to magnetic trap. After the GM phase, optical pumping is applied in 0.8 ms, during which the atoms are pumped to the stretched low field seeking Zeeman state $|F = 2, m_F = 2\rangle$, and are then loaded to the optically plugged magnetic trap. In the loading magnetic trap process, a magnetic trap with lower gradient of about 10 G/cm is first used and then the trap gradient is increased to 200 G/cm in 200 ms. The specially designed ramp stage can prevent the atoms in other low fields seeking hyperfine states from loading to the magnetic trap. Lastly, atoms loaded in the magnetic trap can be probed after a few ms of TOF. The atom number in the magnetic trap as a function of the two-photon Raman detuning in GM is shown in Fig. 4(a). Here, the one-photon detuning is $\Delta = 2.48\Gamma$. We also observe a Fano-like profile, from which the loading efficiency is increased to 70% by the GM cooling mechanism.

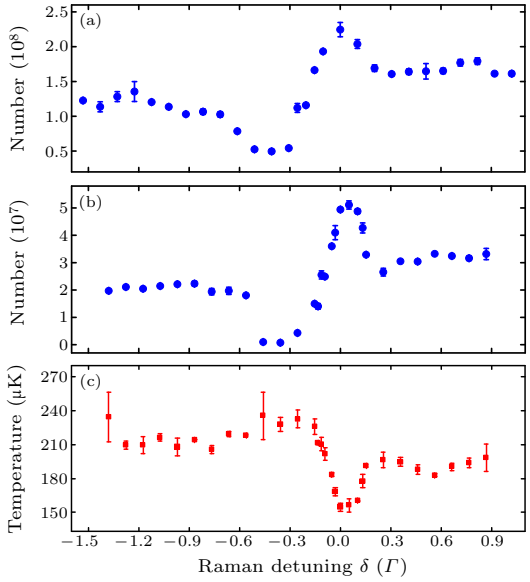

Fig. 4. (a) The atom number loaded into the magnetic trap as a function of the two-photon Raman detuning. The number (b) and temperature (c) of atoms after a short RF forced evaporative cooling as a function of the two-photon Raman detuning in GM phase at $\Delta = 2.48\Gamma$.

After loading to the magnetic trap, an RF forced evaporative cooling is performed to cool the atomic sample down to lower temperature for 5 s. We also study the effect of GM on this stage. The atom number and temperature after evaporative cooling versus the two-photon Raman detuning in GM are shown in Figs. 4(b) and 4(c). After optimizing the parameters on the GM, an atomic sample containing 5.1×10^7 atoms with $T = 150\,\mu$K is produced.

In conclusion, we have shown an effective GM cooling of sodium on the D_2 transition, thanks to the sufficiently large hyperfine split about 6Γ between $|F_e = 2\rangle$ and $|F_e = 3\rangle$ in the excited state $3^2P_{3/2}$, and the phase coherence between the cooling and repumping beams from a single laser source. We have investigated the properties of GM cooling by studying the dependence of the sample temperature on the one-photon detuning, two-photon Raman detuning, molasses duration time and the intensity ratio. The high phase space density after GM provides a starting condition for the effective loading of magnetic traps, which is the best evidence of the cooling mechanism. The experimental results give us a picture of GM for D_2 line, which could work in the atomic species with the hyperfine split about $\sim 6\Gamma$ in excited states. Our experiment shows that GM cooling on the D_2 line is a viable route to high phase space density, while it is lower than in GM cooling on D_1 line. The requirement for only a single laser for all of the cooling process is a clear advantage.

References

[1] Bloch I, Dalibard J and Zwerger W 2008 *Rev. Mod. Phys.* **80** 885
[2] Windpassinger P and Sengstock K 2013 *Rep. Prog. Phys.* **76** 086401
[3] Eckardt A 2017 *Rev. Mod. Phys.* **89** 011004
[4] Gross C and Bloch I 2017 *Science* **357** 995
[5] Qi W, Li Z H and Liang Z X 2018 *Chin. Phys. Lett.* **35** 010301
[6] Galitski V and Spielman I B 2013 *Nature* **494** 49
[7] Goldman N, Juzeliūnas G, Öhberg P and Spielman I B 2014 *Rep. Prog. Phys.* **77** 126401
[8] Zhai H 2015 *Rep. Prog. Phys.* **78** 026001
[9] Liu X J, Hu H and Pu H 2015 *Chin. Phys.* B **24** 050502
[10] Zhang J, Hu H, Liu X and Pu H 2014 *Annu. Rev. Cold At. Mol.* **2** 81
[11] Chai X D, Yu Z F, Zhang A X and Xue J K 2017 *Chin. Phys. Lett.* **34** 090301
[12] Carr L D, DeMille D, Krems R V and Ye J 2009 *New J. Phys.* **11** 055049
[13] Xu R D, Liu W L, Wu J Z, Ma J, Xiao L T and Jia S T 2016 *Acta Phys. Sin.* **65** 093201 (in Chinese)
[14] Moses S A, Covey J P, Miecnikowski M T, Jin D S and Ye J 2017 *Nat. Phys.* **13** 13
[15] Cheuk L W, Nichols M A, Okan M, Gersdorf T, Ramasesh V V, Bakr W S, Lompe T and Zwierlein M W 2015 *Phys. Rev. Lett.* **114** 193001
[16] Parsons M F, Huber F, Mazurenko A, Chiu C S, Setiawan W, Wooley-Brown K, Blatt S and Greiner M 2015 *Phys. Rev. Lett.* **114** 213002
[17] Omran A, Boll M, Hilker T A, Kleinlein K, Salomon G, Bloch I and Gross C 2015 *Phys. Rev. Lett.* **115** 263001
[18] Haller E, Hudson J, Kelly A, Cotta D A, Peaudecerf B, Bruce G D and Kuhr S 2015 *Nat. Phys.* **11** 738
[19] Edge G J A, Anderson R, Jervis D, Mckay D C, Day R, Trotzky S and Thywissen J H 2015 *Phys. Rev.* A **92** 063406
[20] Hu J, Urvoy A, Vendeiro Z, Crépel V, Chen W and Vuletić V 2017 *Science* **358** 1078
[21] Dalibard J and Cohen-Tannoudji C 1989 *J. Opt. Soc. Am.* B **6** 2023

[22] Lett P D, Phillips W D, Rolston S L, Tanner C E, Watts R N and Westbrook C I 1989 *J. Opt. Soc. Am.* B **6** 2084
[23] Weiss D S, Riis E, Shevy Y, Ungar P J and Chu S 1989 *J. Opt. Soc. Am.* B **6** 2072
[24] Aspect A, Arimondo E, Kaiser R, Vansteenkiste N and Cohen-Tannoudji C 1988 *Phys. Rev. Lett.* **61** 826
[25] Grynberg G and Courtois J Y 1994 *Europhys. Lett.* **27** 41
[26] Boiron D, Triché C, Meacher D R, Verkerk P and Grynberg G 1995 *Phys. Rev.* A **52** R3425(R)
[27] Boiron D, Michaud A, Lemonde P, Castin Y, Salomon C, Weyers S, Szymaniec K, Cognet L and Clairon A 1996 *Phys. Rev.* A **53** R3734(R)
[28] Triché C, Verkerk P and Grynberg G 1999 *Eur. Phys. J.* D **5** 225
[29] Esslinger T, Ritsch H, Weidemüller M, Sander F, Hemmerich A and Hänsch T W 1996 *Opt. Lett.* **21** 991
[30] Fernandes D R, Sievers F, Kretzschmar N, Wu S, Salomon C and Chevy F 2012 *Europhys. Lett.* **100** 63001
[31] Sievers F, Kretzschmar N, Fernandes D R, Suchet D, Rabinovic M, Wu S, Parker C V, Khaykovich L, Salomon C and Chevy F 2015 *Phys. Rev.* A **91** 023426
[32] Grier A T, Ferrier-Barbut I, Rem B S, Delehaye M, Khaykovich L, Chevy F and Salomon C 2013 *Phys. Rev.* A **87** 063411
[33] Salomon G, Fouché L, Wang P, Aspect A, Bouyer P and Bourdel T 2013 *Europhys. Lett.* **104** 63002
[34] Nath D, Easwaran R K, Rajalakshmi G and Unnikrishnan C S 2013 *Phys. Rev.* A **88** 053407
[35] Burchianti A, Valtolina G, Seman J A, Pace E, De Pas M, Inguscio M, Zaccanti M and Roati G 2014 *Phys. Rev.* A **90** 043408
[36] Colzi G, Durastante G, Fava E, Serafini S, Lamporesi G and Ferrari G 2016 *Phys. Rev.* A **93** 023421
[37] Chen H, Yao X, Wu Y, Liu X, Wang X, Wang Y, Chen Y and Pan J 2016 *Phys. Rev.* A **94** 033408
[38] Bouton Q, Chang R, Hoendervanger A L, Nogrette F, Aspect A, Westbrook C I and Clément D 2015 *Phys. Rev.* A **91** 061402
[39] Bruce G D, Haller E, Peaudecerf B, Cotta D A, Andia M, Wu S, Johnson M Y H, Lovett B W and Kuhr S 2017 *J. Phys.* B **50** 095002
[40] Rosi S, Burchianti A, Conclave S, Naik D S, Roati G, Fort C and Minardi F 2018 *Sci. Rep.* **8** 1301
[41] Donley E A, Heavner T P, Levi F, Tataw M O and Jefferts S R 2005 *Rev. Sci. Instrum.* **76** 063112
[42] Imai H, Akatsuka T, Ode T and Morinaga A 2012 *Phys. Rev.* A **85** 013633
[43] Tanaka H, Imai H, Furuta K, Kato Y, Tashiro S, Abe M, Tajima R and Morinaga A 2007 *Jpn. J. Appl. Phys.* **46** L492